Available online at www.sciencedirect.com
ScienceDirect
Carbohydrate Research 341 (2006) 2669–2676
Carbohydrate RESEARCH

Structural analysis of a unique hybrid-type ganglioside with *isoglobo*-, *neolacto*-, and *ganglio*-core from the gills of the Pacific salmon (*Oncorhynchus keta*)☆

Yukio Niimura*

Research Center of Biomedical Analysis and Radioisotope, Teikyo University School of Medicine, 2-11-1 Kaga, Itabashi-ku, Tokyo 173-8605, Japan

Received 14 June 2006; received in revised form 13 July 2006; accepted 29 July 2006
Available online 18 September 2006

Abstract—Monosialosyl gangliosides from the gills of the Pacific salmon, *Oncorhynchus keta*, have been prepared by solvent extraction and DEAE-Sephadex column chromatography. The unknown acidic glycolipids (M14 and M15) with slower mobility than GM1a on thin-layer chromatography were separated by Iatrobeads column chromatography and were characterized by compositional analysis, methylation analysis, chemical, and enzymatic degradation, negative-ion LSIMS, and ^{1}H nuclear magnetic resonance spectroscopy. Both M14 and M15 contained a same oligosaccharide core with *isoglobo*-, *neolacto*-, and *ganglio*-series as follows:

α-D-Neu*p*5Ac-(2→3)-β-D-Gal*p*-(1→4)-β-D-Glc*p*NAc-(1→3)-α-D-Gal*p*-(1→3)-β-D-Gal*p*-(1→4)-β-D-Glc*p*-(1↔1)-Cer
3 4
↑ ↑
1 1
α-L-Fuc*p* β-D-Gal*p*NAc

The only difference between M14 and M15 was in fatty acid acylation. Analysis of the fatty acids indicated a predominance of C24:1 fatty acid in M14 and shorter chain saturated fatty acids, C14:0 and C16:0, in M15.

Keywords: *Oncorhynchus keta*; Ganglioside; NMR; Negative-ion LSIMS

1. Introduction

Glycolipids from actively transporting organs such as the kidney of mammals have been studied in detail.[2–7] However, there have been only a few reports on glycolipids from the major osmoregulatory organs of aqueous vertebrates. A unique ganglioside, fucosyl-GalNAc-GM1a, was characterized from the kidney of the salmon.[8] Recently the related disialosyl ganglioside, fucosyl-GalNAc-GD1a, and its *O*-acetyl derivative were also characterized from the same organ.[9] The gills of salmon are known to play important roles in allowing the fish to adapt to river water from sea water during the reproduction season. In addition, it has been reported that the metabolism of sulfatide in the gills of eels were increased when the organism was transferred to sea water from fresh water.[10] The profiles of glycosphingolipids of teleost gills have not been studied to date, although the structures of glycosphingolipids of teleosts were reported from the brain,[11] milt,[12] liver,[13,14] and roe.[15,16] A previous study reported the isolation and characterization of acidic glycosphingolipids from the gills of the Pacific salmon, *Oncorhynchus keta*, which identified a new ganglioside with a hybrid type

☆ The nomenclature system for lipids follows the recommendation of the Nomenclature Committee, International Union of the Pure and Applied Chemistry.[1]

* Tel.: +81 03 3964 3479; fax: +81 03 3964 5807; e-mail: yniimura@med.teikyo-u.ac.jp

0008-6215/$ - see front matter © 2006 Elsevier Ltd. All rights reserved.
doi:10.1016/j.carres.2006.07.016

of *isoglobo* and *neolacto*-series.[17] In this study, a unique ganglioside with another hybrid type core was characterized from the gills of this organism.

2. Experimental

2.1. Materials

The gills were freshly prepared from Pacific salmon captured off the Sanriku Coast in Japan in December. The material was frozen at −40 °C until use. Glycosphingolipid standard compounds, chemicals, and reagents were as described previously.[17] β-Galactosidase (EC 3.2.1.23, grade VII) and β-*N*-acetyl-hexosaminidase (EC 3.2.1.30) from jack bean, α-galactosidase (EC 3.2.1.22) from green beans, and neuraminidase (EC 3.2.1.18, type V) from *Clostridium perfringens* were from Sigma, St. Louis, USA. Reagents for derivatization or NMR spectroscopy were used as previously described.[18]

2.2. Thin-layer chromatography

Thin-layer chromatography (TLC) was performed on Silica Gel 60 high performance TLC (HPTLC) plates (E, Merck, Darmstadt, Germany) with the following solvent systems: I, $CHCl_3/CH_3OH/0.2\%CaCl_2$ (55:45:10, v/v); II, $CHCl_3/CH_3OH/H_2O$ (60:35:8, v/v); and III, $CHCl_3/CH_3OH/3.5$ N NH_4OH (55:45:10, v/v). Glycolipids were visualized by spraying the plate with orcinol/H_2SO_4 reagent or resorcinol reagent[19] and heating for 5 min at 120 °C.

2.3. Lipid extraction and purification of the gangliosides

Lipid extraction from 550 g of gills and separation of acidic glycolipids on DEAE-Sephadex A-25 column chromatography was carried out as described previously.[17] The fractions corresponding to the monosialosyl glycolipids were collected and the purification of glycolipids was further performed by high performance liquid chromatography (HPLC) with a Shimadzu LC 4A apparatus using a column (1 × 30 cm) of Iatrobeads (6RS-8005) with $CHCl_3/CH_3OH/H_2O$ (60:40:2, v/v) at the flow rate of 1 mL/min. This procedure produced the pure compounds M14 and M15.

2.4. Chemical and spectral analyses

Monosaccharides, fatty acids, and sphingoids were analyzed by gas–liquid chromatography (GLC) as described.[17] Negative-ion liquid secondary ion mass-spectrometry (LSIMS) was performed with Concept 1H spectrometer (Shimadzu/Kratos, Kyoto, Japan) fitted with a cesium ion gun. About 0.5 nmol of underivatized glycolipid was mixed with 1 μL triethanolamine as the matrix. Spectra were recorded at an accelerating voltage of 8 kV, with a scan rate of 5 s/decade, and at a resolution of 1000–2000. For the measurement of ^1H nuclear magnetic resonance (NMR) spectroscopy, the purified glycolipids were treated repeatedly with 0.5 mL portions of $CH_3O[^2H]$, followed by desiccation over P_2O_5 in vacuo to exchange the exchangeable protons with deuterium. The dried glycolipids were redissolved in 0.5 mL of a mixture of [^2H]dimethyl sulfoxide/$[^2H]_2O$ (98:2, v/v). The spectra were recorded on a 400 MHz spectrometer GX-400 of Japan Electron Optical Laboratory (JEOL, Tokyo, Japan) at 60 °C. The operation conditions for one-dimensional spectrum were as follows: frequency, 400 MHz; sweep width, 4 kHz; sampling points, 16k. All two-dimensional spectra were recorded with 512 × 2048 data points and a spectral width of 2500 Hz as previously described.[18] Chemical shifts (ppm) were referenced from the signal of tetramethylsilane (TMS) as an internal standard.

2.5. Methylation analysis

The glycolipid was methylated,[20,21] acetolyzed,[22] reduced with $NaB[^2H]_4$,[23] and acetylated according to published procedures.[24] The acetates of partially methylated, 6-deoxyhexitol, hexitol, and hexosaminitol were analyzed by gas–liquid chromatography–mass spectrometry (GLC–MS) as described.[17] A mass range from 45 to 450 atomic mass units was scanned every 6 s. Peaks were identified by retention times and by characteristic fragment ions. Mass fragment patterns of terminal sugar ions were used to calculate the yields of methylated glycolipids. For cerebroside, *m*/*z* 187 (Hex–CH_3OH) was measured at an ion-source temperature of 250 °C, *m*/*z* 344 (NeuNAc–CH_3OH) for GM3 at 280 °C, and *m*/*z* 260 (HexNAc) for globoside at 285 °C.

2.6. Limited degradation of glycolipid

The purified glycolipid was treated with 1% trichloroacetic acid at 100 °C for 1 h.[17] Treatment of glycolipids with β-galactosidase from Jack beans was performed as described.[8] In the case of β-*N*-acetylhexosaminidase from Jack beans, a sodium citrate buffer at pH 5.0 was used and α-galactosidase from green beans was used with sodium taurocholate (1 mg/mL) in a sodium citrate buffer at pH 4.0. The reaction mixture was adjusted to $CHCl_3/CH_3OH/H_2O$ (30:60:8, v/v), and the product purified as described.[8]

3. Results

3.1. Preparation of unknown monosialosyl gangliosides M14 and M15 from the gills of salmon

Acidic glycolipids were eluted from DEAE-Sephadex A-25 by increasing the concentration of TEAB (triethyl-

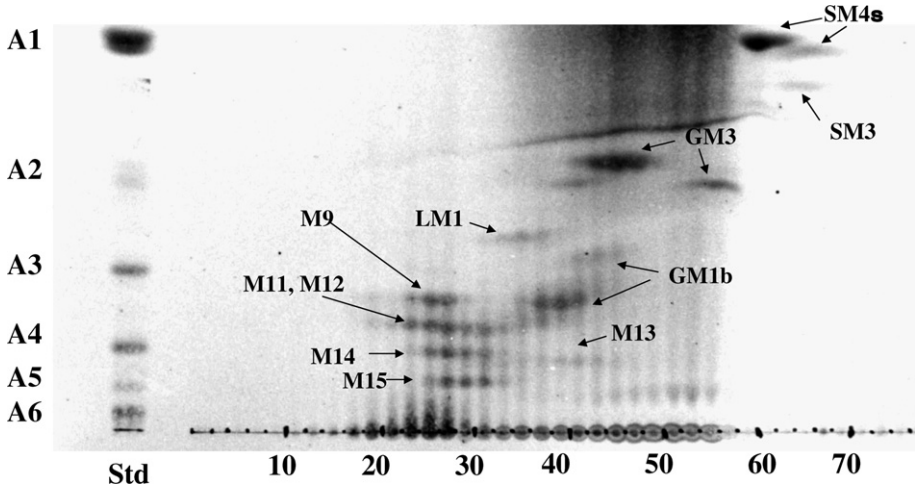

Figure 1. Elution profile of monosialosyl gangliosides and sulfoglycolipids of salmon gills from a DEAE-Sephadex A-25 column. Acidic glycolipids were separated on a DEAE-Sephadex A-25 (bicarbonate form, 1.2×45 cm) column with the linear gradient system from $CHCl_3/CH_3OH/H_2O$ (30:60:8, v/v) to $CHCl_3/CH_3OH$/0.8 M TEAB (triethylamine carbonate) (30:60:8, v/v). Solvent system I ($CHCl_3/CH_3OH$/0.2% $CaCl_2$, 55:45:10, v/v) was used for HPTLC. Glycolipid bands were visualized on a HPTLC plate using the orcinol/H_2SO_4 spray. SM4s: GalCer I^3 sulfate; SM3: LacCer II^3-sulfate; GM3: II^3αNeuNAc-LacCer; GM1b: IV^3αNeuNAc-Gg_4Cer; LM1: IV^3αNeuNAc-nLc_4Cer; M9 and M12: fucosyl-GalNAc-GM1a; M11 and M1: α-D-Neu*p*NAc-(2→3)-β-D-Gal*p*-(1→4)[α-L-Fuc*p*-(1→3)]-β-D-Glc*p*NAc-(1→3)-α-D-Gal*p*-(1→3)-β-D-Gal*p*-(1→4)-β-D-Glc*p*-(1↔1)-Cer; M14 and M15: unknown glycolipids; standard lane: a mixture of rat brain acidic glycosphingolipids for reference. A1: SM4s; A2: GM3; A3: GM1a (II^3αNeuNAc-Gg_4Cer); A4: GD1a; A5: GD1b; A6: GT1b + GQ1b.

amine carbonate). The major acidic glycolipids containing a unique hybrid type ganglioside were isolated and characterized.[17] In addition, two unknown bands (M14 and M15) were detected by TLC in the faster eluting column fractions containing monosialosyl gangliosides (Fig. 1). These glycolipids were purified by HPLC on an Iatrobeads column to single bands on TLC plates with solvent systems I and II (Fig. 2). These acidic glycolipids appeared to be gangliosides because of their reactivity with orcinol/H_2SO_4 and resorcinol/HCl.

3.2. Compositional analysis of gangliosides M14 and M15

Both M14 and M15 contained glucose (Glc), galactose (Gal), *N*-acetylgalactosamine (GalNAc), *N*-acetylglucosamine (GlcNAc), fucose (Fuc), and *N*-acetylneuraminic acid (NeuNAc) at the approximate proportion of 1:3:1:1:1:1 (Table 1). NeuNAc was detected as a species of sialic acid in both gangliosides. The major fatty acids were C16:0, C18:0, and C24:1 in M14, while C14:0 and C16:0 were present in M15. The long chain bases found in M14 were 4-sphingenine (d18:1) and 4-hydroxysphinganine (t18:0); and M15 contained d18:1 and 4-sphinganine (d18:0).

3.3. Enzyme degradation

M15 is sensitive to neuraminidase of *Clostridium perfringens*, and therefore the *N*-acetylneuraminic acid residue is linked to the non-reducing terminus of the molecule. The desialylated product of M15 was further degraded with trichloroacetic acid to produce defucosylated glycolipid. This product could also be degraded sequentially by β-galactosidase, β-*N*-acetylhexosaminidase, α-galactosidase, β-*N*-acetylhexosaminidase, and β-galactosidase to give a monohexosylceramide finally. After treatment with α-galactosidase, reaction with β-*N*-acetylhexosaminidase was necessary to obtain a dihexosylceramide (Fig. 3). Based on these results, the core structure of M15 was proposed to be:

α-D-Neu*p*5Ac-β-D-Gal*p*-β-D-Glc*p*NAc-α-D-Gal*p*[β-D-Gal*p*NAc-]β-D-Gal*p*-β-D-Glc*p*-Cer

or

α-D-Neu*p*5Ac-β-D-Gal*p*-β-D-Glc*p*NAc-α-D-Gal*p*-β-D-Gal*p*NAc-β-D-Gal*p*-β-D-Glc*p*-Cer

3.4. Methylation analysis

From the methylation analysis of intact M15, the alditol acetates 2,3,6-*O*-methylglucitol, 2,4,6-*O*-methylgalactitol, 2,6-*O*-methylgalactitol, 2,3,4-*O*-methyl-6-deoxygalactitol, 6-*O*-methyl-*N*-acetylglucosaminitol, and 3,4,6-*O*-methyl-*N*-acetylgalactosaminitol were detected at the approximate proportion of 1:2:1:1:1:1 (Table 2). From these results glycoside linkages were proposed to be:

α-D-Neu*p*5Ac-(2→3)-β-D-Gal*p*-(1→3 or 4)-β-D-Glc*p*NAc-(1→3)-α-D-Gal*p*-(1→3 or 4)-β-D-Gal*p*-(1→4)-β-D-Glc*p*-(1↔1)-Cer

3 or 4 ↑ 1 α-L-Fuc*p*

3 or 4 ↑ 1 β-D-Gal*p*NAc

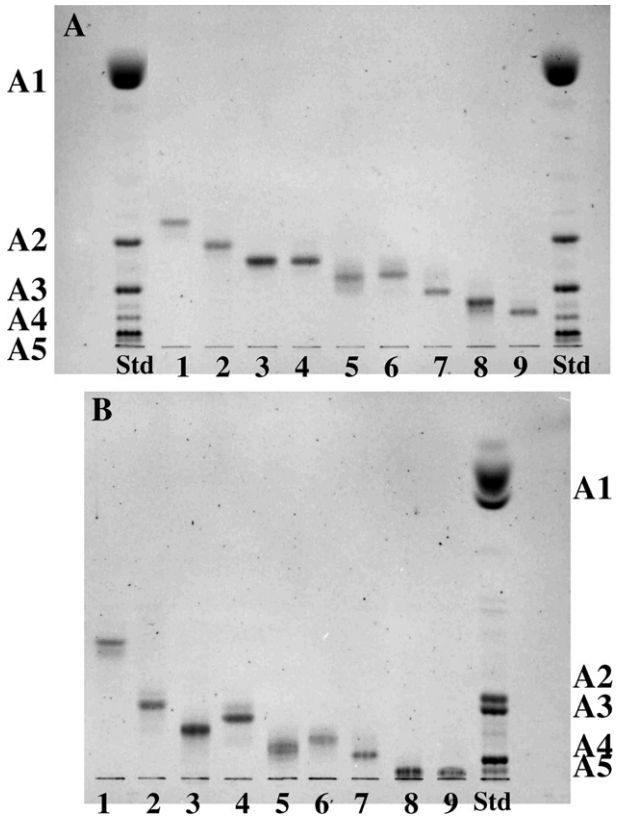

Figure 2. HPTLC pattern of gangliosides purified from salmon gill. TLC was performed with solvent system I ($CHCl_3/CH_3OH$/0.2% $CaCl_2$, 55:45:10, v/v) in panel A and III ($CHCl_3/CH_3OH$/3.5 N NH_4OH, 55:45:10, v/v) in panel B, respectively. Standard Lane: rat brain acidic glycosphingolipids (cf. Fig. 1); lane 1: LM1; lane 2: GM1b (upper band); lane 3: fucosyl-GalNAc-GM1a (upper band); lane 4: GM1b (lower band); lane 5: α-D-Neu*p*NAc-(2→3)-β-D-Gal*p*-(1→4)-[α-L-Fuc*p*-(1→3)]-β-D-Glc*p*NAc-(1→3)-α-D-Gal*p*-(1→3)-β-D-Gal*p*-(1→4)-β-D-Glc*p*-(1↔1)-Cer (upper band); lane 6: fucosyl-GalNAc-GM1a (lower band); lane 7: α-D-Neu*p*NAc-(2→3)-β-D-Gal*p*-(1→4)-[α-L-Fuc*p*-(1→3)]-β-D-Glc*p*NAc-(1→3)-α-D-Gal*p*-(1→3)-β-D-Gal*p*-(1→4)-β-D-Glc*p*-(1↔1)-Cer (lower band); lane 8: M14; lane 9: M15. The orcinol reagent was used for detection.

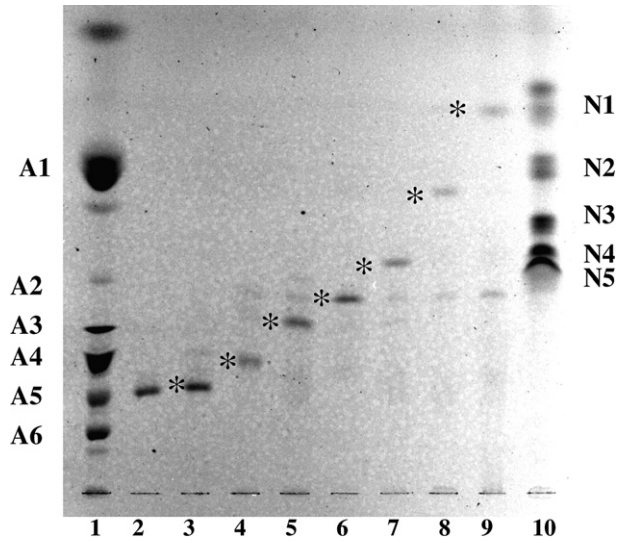

Figure 3. Sequential degradation of ganglioside M15. Lane 1: rat brain acidic glycolipid (cf. Fig. 1); lane 2: purified M15; lane 3: product of M15 treated with neuraminidase; lane 4: product of lane 3 treated with trichloroacetic acid; lane 5: product of lane 4 incubated with β-galactosidase from jack bean; lane 6: product of lane 5 incubated with β-*N*-acetylhexosaminidase from jack bean; lane 7: product of lane 6 incubated with α-galactosidase from jack bean; lane 8: product of lane 7 incubated with β-*N*-acetylhexosaminidase from jack bean; lane 9: product of lane 8 incubated with β-galactosidase from jack bean; lane 10: neutral glycolipid mixture from horse kidney as standards; N1: monohexosyl ceramide; N2: dihexosyl ceramide; N3: Gb_3Cer; N4: Gb_4Cer; N5: Gb_5Cer. The HPTLC plate was developed with solvent system II.

Further methylation analysis was performed on the desialylated and defucosylated product. Because 3,6-*O*-methyl-*N*-acetylglucosaminitol was detected, the presence of the β-D-Gal*p*-(1→4)-β-D-Glc*p*NAc-linkage was established. Therefore, the β-D-Gal*p*-(1→4)[α-L-Fuc*p*-(1→3)]-β-D-Glc*p*NAc-linkage was confirmed in native core structure. The other degradation product, β-D-Gal*p*NAc-β-D-Gal*p*-β-D-Gal*p*-Cer, was also prepared from the desialylated and defucosylated product by further stepwise hydrolysis with β-galactosidase, β-*N*-acetylhexosaminidase, and α-galactosidase. As 2,3,6-*O*-methylgalactitol was detected on a SP2340 column by methylation analysis of this product, the linkage of β-D-Gal*p*NAc-(1→4)-β-D-Gal*p*- was confirmed. Because the product corresponding to α-D-Gal*p*-β-D-Gal*p*-β-D-Gal*p*-Cer was not observed on TLC from the above stepwise hydrolysis (lane 7 in Fig. 3), it was ruled out that 2,3,6-*O*-methylgalactitol arose from an α-D-Gal*p*-(1→4)-β-D-Gal*p*-linkage. The α-D-Gal*p*-(1→3)[β-D-Gal*p*NAc-(1→4)]-β-D-Gal*p*-linkage was also determined as the core structure. From these results the glycoside linkage of M15 was proposed as follows:

α-D-Neu*p*5Ac-(2→3)-β-D-Gal*p*-(1→4)-β-D-Glc*p*NAc-(1→3)-α-D-Gal*p*-(1→3)-β-D-Gal*p*-(1→4)-β-D-Glc*p*-(1↔1)-Cer

3 ↑ 1 α-L-Fuc*p*

4 ↑ 1 β-D-Gal*p*NAc

Table 1. Compositional analyses of M14 and M15[a]

	Carbohydrate					
	Glc	Gal	GalNAc	GlcNAc	Fuc	NeuNAc
M14	1.00	3.00	0.92	0.81	0.58	0.54
M15	1.00	2.96	1.03	1.03	0.64	0.75

	Fatty acid (%)						Long chain bases (%)		
	C14:0	C16:0	C18:0	C18:1	C24:1	Others	d18:1	d18:0	t18:0
M14	—	32.7	37.0	6.7	23.5	—	61	—	39
M15	31.1	44.6	17.1	—	—	7.2	71	20	9

[a] Carbohydrate molar ratios were calculated based on the GLC peak areas of methylated glycosides using methylated fucosyl GM1a and sialosylparagloboside as calibration standards. Fatty acids and long chain bases were identified by the retention time and the peak areas on capillary column of GLC.

Table 2. Partially-O-methylated hexitol and hexosaminitol acetates derived from the permethylated intact gangliosides[a]

	2,3,6-Glc	2,4,6-Gal	2,6-Gal	3,4,6-GalNAc	6-GlcNAc	2,3,4-Fuc
M13	1.00	2.59	—	—	0.99	0.63
M15	1.00	1.67	1.11	0.67	0.55	0.65

[a] The M13 glycolipid, which lacks the GalNAc residue in M15 was used as a control;[17] values were determined by GLC on a CBP-1 capillary column; molar ratios of alditol acetates are related to 1,4,5-tri-*O*-acetyl-2,3,6-tri-*O*-methylglucitol (2,3,6-Glc).

3.5. Negative-ion LSIMS

Negative-ion liquid secondary ion mass spectroscopy (LSIMS) of M15 showed an intense pseudomolecular ion $[M-H]^-$ at *m/z* 2017 corresponding to the ceramide species of (t18:0/C14:0), a week ion $[M-H]^-$ at *m/z* 1999 to (d18:1/C14:0) and other characteristic fragment ions (Fig. 4). Fragment ions were detected at *m/z* 526 [ceramide, t18:0/14:0]$^-$, 688 [monohexosylceramide]$^-$, 850 [dihexosylceramide]$^-$, 1053 [tetrahexosylceramide]$^-$, 1215 [M−H−NeuNAc−Hex−dHex]$^-$, 1418, 1564 [M−H−NeuNAc−Hex]$^-$, and 1726 [M−H−NeuNAc]$^-$, respectively. *M/z* 1506, 1344, and 979 were assigned to the corresponding the glycans as shown in Figure 4.

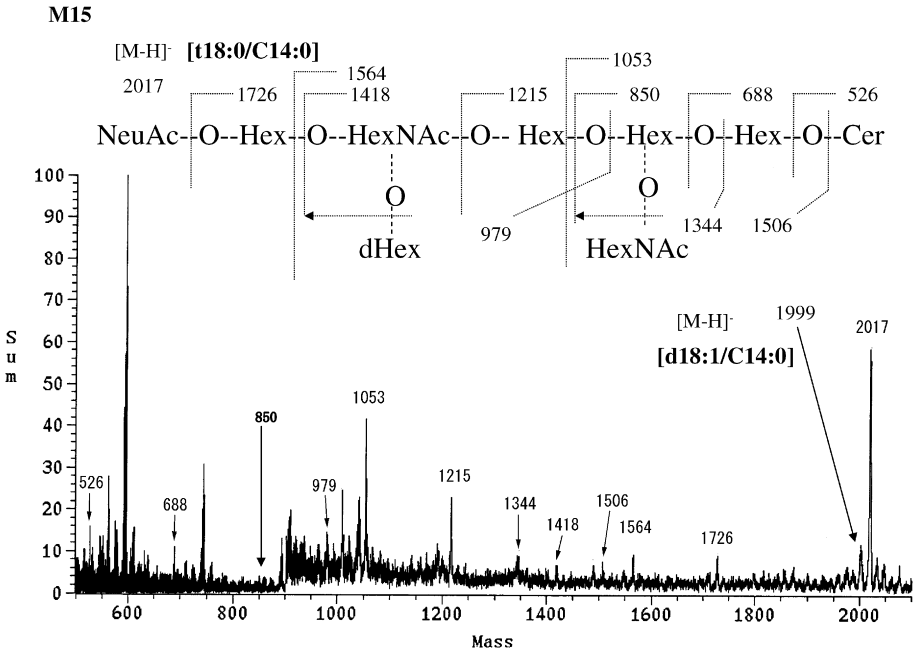

Figure 4. Negative-ion LSIMS of M15. Mass numbers indicated in the spectrum are characteristic signals. The peaks in the mass range higher than when *m/z* 900 was amplified 5-fold. The values of *m/z* are represented by nominal masses omitting the decimal fractions.

3.6. NMR study

One-dimensional ^{1}H NMR spectroscopy of M15 (Fig. 5A) showed a doublet for H-1 of Fuc(VII), Gal-(III), GlcNAc(IV), GalNAc(VI), Gal(II), Gal(V), and Glc(I) at 4.92 ppm ($J = 3.9$ Hz), 4.96 ppm ($J = 3.9$ Hz), 4.70 ppm ($J = 7.8$ Hz), 4.45 ppm ($J = 8.8$ Hz), 4.33 ($J = 7.8$ Hz), 4.28 ppm ($J = 7.8$ Hz), and 4.18 ppm ($J = 7.8$ Hz), respectively. A quartet for H-5 of Fuc at 4.61 ppm, and a quartet for H-3eq of NeuNAc(VIII) at 2.774 ppm and a doublet for H-6 of Fuc at 1.02 ppm ($J = 6.8$ Hz) were also detected (Fig. 5A and Table 3). The signal for H-1 of Gal(II) (4.33 ppm) may be shifted to the lower field than the same

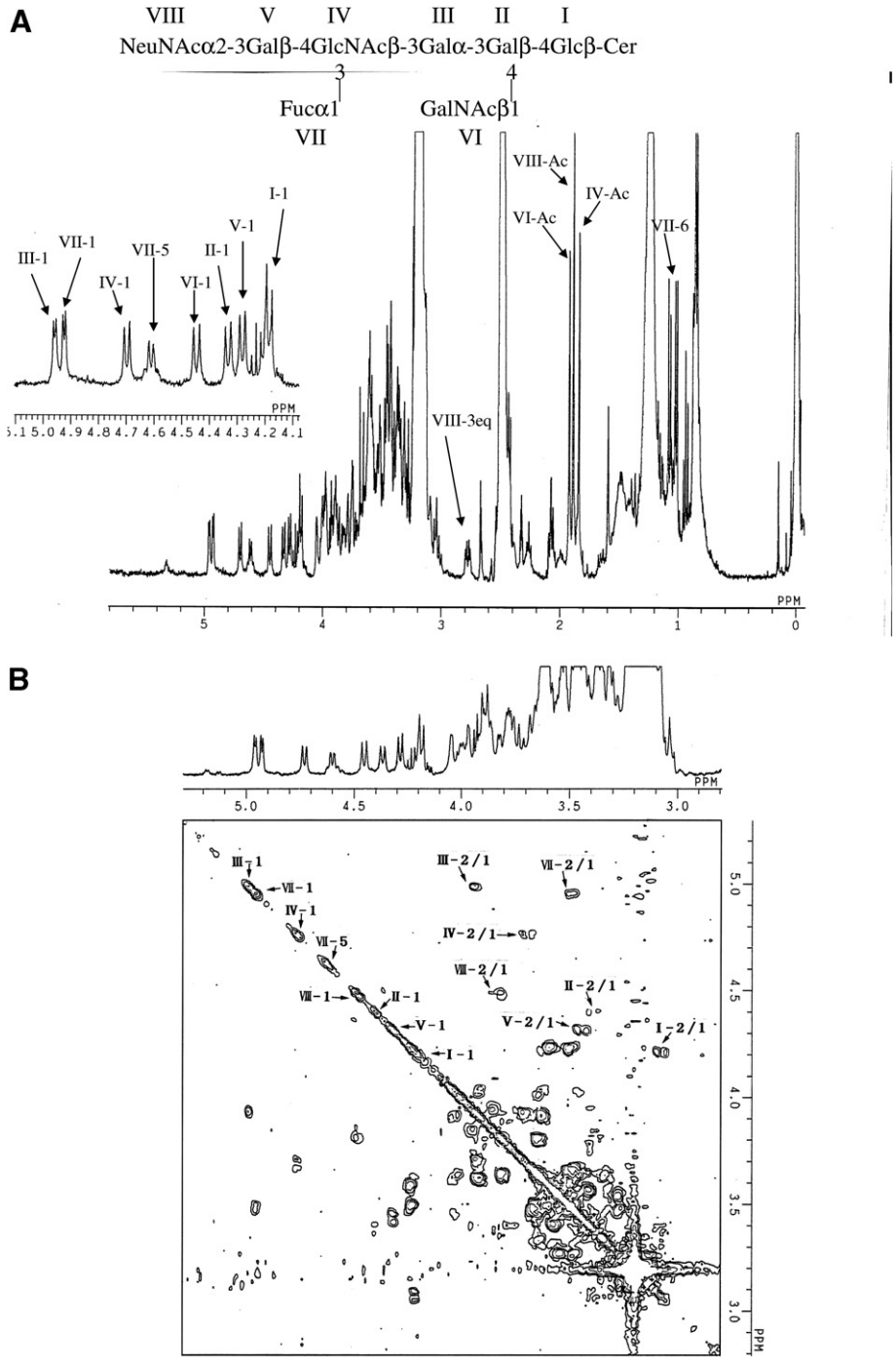

Figure 5. Proton magnetic resonance spectrum of ganglioside M15. Chemical shifts (ppm) are referenced relative to TMS as an internal standard. (Panel A) Anomeric region in one-dimensional spectrum. Arabic numbers refer to ring protons of sugar residues marked by Roman numerals in structure drawn in Table 3. (Panel B) Two-dimensional COSY spectrum of M15.

Table 3. Chemical shifts (ppm) and coupling constants (J) in parenthesis of new gangliosides

VIII V IV III II I
NeuNAcα2-3Galβ-4GlcNAcβ-3Galα-3Galβ-4Glcβ-Cer
3 4
Fucα1 GalNAcβ1
VII VI

	VIII-3eq	VII-6	VII-5	VII-1	VI-1	V-1	IV-1	III-1	II-1	I-1
M14	2.72	1.02 (6.8)	4.60	4.93 (3.0)	4.45 (7.8)	4.29 (7.8)	4.73 (6.8)	4.96 (3.9)	4.38 (6.8)	4.18 (7.8)
M15	2.774	1.02 (6.8)	4.61	4.93 (3.9)	4.45 (8.8)	4.28 (7.8)	4.697 (7.8)	4.959 (3.9)	4.331 (7.8)	4.184 (7.8)

signal (4.31 ppm) in M13[17] due to the attachment of GalNAc.

The *N*-acetylmethyl protons of NeuNAc, GlcNAc, and GalNAc were observed at 1.89, 1.84, and 1.92 ppm, respectively, as singlets. The two-dimensional chemical shift correlation spectroscopy (COSY) spectrum of M15 revealed the coupling of H-1/H-2 in hexoses and β-*N*-acetylhexosamines (Fig. 5B). The NMR spectrum of M14 (data not shown) also showed signals similar to the saccharide chain of M15. The signals arising from the *cis*-olefin methines of the unsaturated fatty acids in M14 (~5.33 ppm) were much larger than those in M15.

4. Discussion

Based on the above results, M14 has the same oligosaccharide structure as M15. There are differences only in the ceramide moiety, where longer chain and unsaturated fatty acids are found in M14, while shorter chain and saturated fatty acids are identified in M15. The partial core structures of α-D-Gal*p*-(1→3)-β-Gal*p*-(1→4)-β-D-Glc*p*-, β-D-Gal*p*-(1→4)-β-D-Glc*p*NAc-, and β-D-Gal*p*-NAc-(1→4)-β-Gal*p*-(1→4)-β-D-Glc*p*- corresponded to *isoglobo*-, *neolacto*-, and *ganglio*-series of ganglioside, respectively. Therefore, these gangliosides belong to a novel sialosylheptaglycosylceramide with a hybrid type structure of the *isoglobo-neolacto-ganglio*-series. The unique hybrid type ganglioside with *isoglobo- and neolacto-core* was previously reported from the gills of salmon.[17] A novel Forssman active acidic glycosphingolipid with branched *isoglobo*-, *ganglio*-, and *neolacto*-series hybrid sugar chains was also characterized from equine kidney.[25] The gangliosides of *ganglio*-series are commonly found in neuronal tissue. The biosynthesis of these gangliosides in the non-neuronal tissues of teleosts may be achieved by their respective glycosyltransferases. The process will be elucidated by analysis of the glycosyltransferase genes that produce these novel gangliosides. In fish gills, the mitochondrion-rich cells, which are interspersed among pavement cells, are important osmoregulatory sites in maintaining ionic balance.[26] Tissue concentrations of M14 and M15 were 1.5 and 1.8 μmol/kg wet weight, respectively. It will be interesting to determine how these glycolipids are distributed in these cell types and how they are presented on the cell surface.

Acknowledgments

The author wishes to thank Mrs. Michiko Ogawa for technical assistance, Dr. Keiko Tadano-Aritomi for measurement of negative-ion LSIMS, Dr. Naoko Tanaka for measurement of NMR spectra and Professor Ineo Ishizuka for encouragement.

References

1. IUPAC-IUB Joint Commission on Biochemical Nomenclature (JCBN). *Glycoconjugate J.* **1999**, *16*, 1–6.
2. Ishizuka, I.; Tadano, K.; Nagata, N.; Niimura, Y.; Nagai, Y. *Biochim. Biophys. Acta* **1978**, *541*, 467–482.
3. Nagai, K.; Tadano-Aritomi, K.; Kawaguchi, K.; Ishizuka, I. *J. Biochem. (Tokyo, Jpn.)* **1985**, *98*, 545–559.
4. Nagai, K.; Ishizuka, I.; Oda, S. *J. Biochem. (Tokyo, Jpn.)* **1984**, *95*, 1501–1511.
5. Niimura, Y.; Ishizuka, I. *J. Biochem. (Tokyo, Jpn.)* **1986**, *100*, 825–835.
6. Niimura, Y.; Ishizuka, I. *Biochim. Biophys. Acta* **1990**, *1052*, 248–254.
7. Niimura, Y.; Ishizuka, I. *Comp. Biochem. Physiol.* **1991**, *100B*, 535–541.
8. Niimura, Y.; Tomori, M.; Tadano-Aritomi, K.; Toida, T.; Ishizuka, I. *J. Biochem. (Tokyo, Jpn.)* **1999**, *126*, 962–968.
9. Niimura, Y.; Ishizuka, I. *Glycoconjugate J.* **2006**, *23*, 487–497.
10. Zwingelstein, G.; Portoukalian, J.; Rebel, G.; Brichon, G. *Comp. Biochem. Physiol.* **1980**, *65B*, 555–558.
11. Ishizuka, I.; Wiegandt, H. *Biochim. Biophys. Acta* **1972**, *260*, 279–289.
12. Ueno, K.; Ishizuka, I.; Yamakawa, T. *J. Biochem. (Tokyo, Jpn.)* **1975**, *77*, 1223–1232.
13. Ostrander, G. K.; Levery, S. B.; Hakomori, S.; Holmes, E. H. *J. Biol. Chem.* **1988**, *263*, 3103–3110.
14. Ostrander, G. K.; Levery, S. B.; Eaton, H. L.; Salyan, M. E. K.; Hakomori, S.; Holmes, E. H. *J. Biol. Chem.* **1988**, *263*, 18716–18725.

15. Li, Y.-T.; Hirabayashi, Y.; DeGasperi, R.; Yu, R. K.; Ariga, T.; Koerner, T. A. W.; Li, S.-C. *J. Biol. Chem.* **1984**, *259*, 8980–8985.
16. DeGasperi, R.; Koerner, T. A. W.; Quarles, R. H.; Ilyas, A. A.; Ishikawa, Y.; Li, S.-C.; Li, Y.-T. *J. Biol. Chem.* **1987**, *262*, 17149–17155.
17. Nimura, Y. *Glycoconjugate J.*, in press.
18. Iida, N.; Toida, T.; Kushi, Y.; Handa, S.; Fredman, P.; Svennerholm, L.; Ishizuka, I. *J. Biol. Chem.* **1989**, *264*, 5974–5980.
19. Svennerholm, L. *Biochim. Biophys. Acta* **1957**, *24*, 604–611.
20. Hakomori, S. *J. Biochem. (Tokyo, Jpn.)* **1965**, *55*, 205–208.
21. Stellner, K.; Watanabe, K.; Hakomori, S. *Biochemistry* **1973**, *12*, 656–661.
22. Nakamura, K.; Hashimoto, Y.; Suzuki, M.; Suzuki, A.; Yamakawa, T. *J. Biochem. (Tokyo, Jpn.)* **1984**, *96*, 949–957.
23. Tadano, K.; Ishizuka, I. *J. Biol. Chem.* **1982**, *257*, 1482–1490.
24. Levery, S. B.; Hakomori, S. *Methods Enzymol.* **1987**, *138*, 13–25.
25. Yamamoto, H.; Iida-Tanaka, N.; Kasama, T.; Ishizuka, I.; Kushi, Y.; Handa, S. *J Biochem (Tokyo, Jpn.)* **1999**, *125*, 923–930.
26. Evans, D. H.; Piermarini, P. M.; Choe, K. P. *Physiol. Rev.* **2005**, *85*, 97–177.